Refereed Proceedings

The 13th International Conference on Fluidization - New Paradigm in Fluidization Engineering

Engineering Conferences International *Year* 2010

THE INFLUENCE OF PARTICLE ATTRITION ON SORBENT INVENTORY AND PARTICLE SIZE DISTRIBUTION IN AIR-BLOWN CIRCULATING FLUIDIZED BED COMBUSTORS

Piero Salatino* Fabio Montagnaro†

Fabrizio Scala‡ Massimo Urciuolo**

*Università degli Studi di Napoli Federico II, Italy, piero.salatino@unina.it

†Università degli Studi di Napoli Federico II, fabio.montagnaro@unina.it

‡Istituto di Ricerche sulla Combustione, Consiglio Nazionale delle Ricerche, scala@irc.cnr.it

**Istituto di Ricerche sulla Combustione, Consiglio Nazionale delle Ricerche, murciuol@unina.it

THE INFLUENCE OF PARTICLE ATTRITION ON SORBENT INVENTORY AND PARTICLE SIZE DISTRIBUTION IN AIR-BLOWN CIRCULATING FLUIDIZED BED COMBUSTORS

Piero Salatino[a,b], Fabio Montagnaro[c], Fabrizio Scala[b], Massimo Urciuolo[b]

[a] Dipartimento di Ingegneria Chimica, Università degli Studi di Napoli Federico II, Piazzale Vincenzo Tecchio 80, 80125 Naples (Italy),
T: +39-081-7682258; F: +39-081-5936936; E: piero.salatino@unina.it

[b] Istituto di Ricerche sulla Combustione, Consiglio Nazionale delle Ricerche, Piazzale Vincenzo Tecchio 80, 80125 Naples (Italy)
T: +39-081-7682969; F: +39-081-5936936; E: scala@irc.cnr.it; murciuol@unina.it

[c] Dipartimento di Chimica, Università degli Studi di Napoli Federico II, Complesso Universitario del Monte di Sant'Angelo, 80126 Naples (Italy)
T: +39-081-674029; F: +39-081-674090; E: fabio.montagnaro@unina.it

ABSTRACT

This paper presents a population balance model aiming at the prediction of sorbent inventory and particle size distribution establishing at steady state in the bed of an air-blown circulating fluidized bed combustor fuelled with a sulphur-bearing solid fuel. The core of the model is represented by population balance equations on sorbent particles which embody terms expressing the extent/rate of sorbent attrition/fragmentation. The effect of the progress of sulphation on attrition and fragmentation is taken into account by selection of appropriate constitutive equations. Model results are presented and discussed with the aim of clarifying the influence of particle attrition/fragmentation on sorbent inventory and particle size distribution, partitioning of sorbent between fly and bottom ash, sulphur capture efficiency. A sensitivity analysis is carried out with reference to relevant operational parameters of the combustor.

INTRODUCTION

Substantial changes in the particle size distribution of limestone-based SO_2 sorbents can be brought about by particle attrition/fragmentation in fluidized bed combustors (FBC). The mutual interference between chemical reactions (calcination and dehydration, sulphation) and attrition/fragmentation of limestone has been largely disclosed (1-13). It has been shown that ***primary fragmentation*** occurs immediately after the injection of sorbent particles in the hot bed, as a consequence of thermal stresses and internal overpressures due to release of gas (CO_2 following calcination of raw sorbent, steam following dehydration of spent/reactivated sorbent). Primary fragmentation takes place in the dense bed/splashing region of FBC reactors, resulting in the generation of coarse and fine fragments. Further

***Table 1*. Main features of attrition/fragmentation mechanisms.**

Mechanism	Caused by…	Location:	Generation of…
Primary fragmentation (decrepitation)	thermal/mechanical stresses	dense bed/ splashing zone	coarse/fine fragments
Attrition by abrasion (surface wear)	rubbing of bed solids	dense bed	fine fragments
Secondary fragmentation (impact fragmentation)	collisions against targets	jetting region + riser exit/cyclone	coarse/fine fragments

breakage occurs as a consequence of mechanical stresses experienced by the particles during their lifetime in the reactor. ***Attrition by abrasion*** is related to the occurrence of surface wear as the emulsion phase of the FB is sheared by the passage of bubbles, and generates fine fragments that are quickly elutriated. ***Secondary fragmentation*** gives rise to coarse and fine fragments, and may onset as a result of high-velocity impacts of sorbent particles against targets (bed material, reactor walls/internals); these impacts are likely experienced by the particles in the jetting region of FBC. The exit region of the riser and the cyclone are other potential locations of impact damage of sorbent particles in a circulating FBC (CFBC) reactor. The main features of attrition/fragmentation mechanisms are summarized in *Table 1* and a conceptual framework for analyzing the effects of particle sulphation/attrition/fragmentation on the fate of sorbents is represented in *Figure 1a*, where the simplification of lumping sorbent particles into *coarse* and *fine* and the population of sorbent particles (of different age and sulphation degree) into *lime* and *sulphated limestone* components has been adopted.

In this work a population balance model is presented, which aims at predicting the sorbent inventory and particle size distribution, the partitioning of sorbent between fly and bottom ash and the sulphur capture efficiency during steady operation of an air-blown CFBC. The influence of attrition/fragmentation on the main output parameters is assessed.

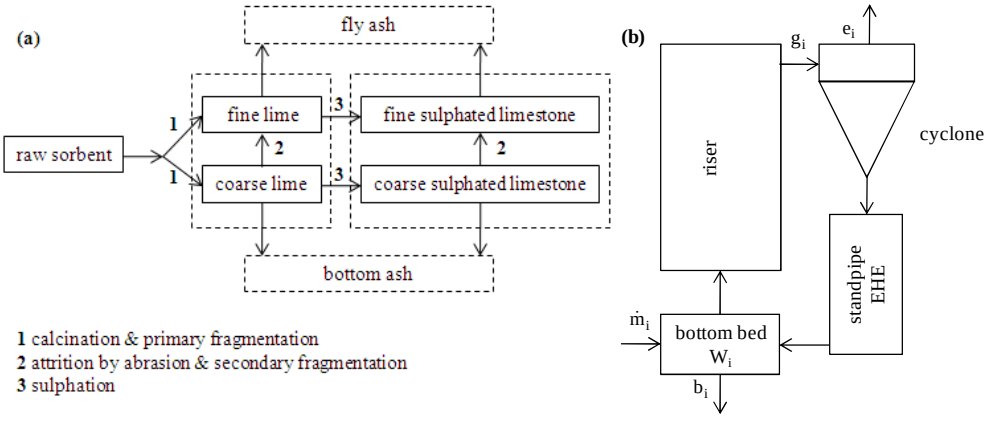

***Figure 1.* (a) Particle sulphation/attrition/fragmentation network for the assessment of the fate of sorbents; (b) Schematic representation of the CFBC loop with the indication of relevant sorbent fluxes.**

MODEL

A schematic representation of the CFBC loop with the indication of relevant sorbent fluxes is reported in *Figure 1b*. Population balance equations can be written on the sorbent present at steady state in the combustor. Calcination and primary fragmentation are assumed to occur almost instantaneously so that the inventory of the raw limestone can be neglected. Each particle in the population is characterized by two variables: the particle size (d) and the sulphation degree (X_S). A simplified version of the population balance is hereby developed based on the assumption that the sorbent can be lumped into two classes as far as X_S is concerned: the unconverted lime (L) and the sulphated limestone (SL). Accordingly, the population balance in the d-X_S domain simplifies yielding two 1-D equations in the d-domain. Upon discretization of the domain and referring to the i-th particle size bin, equations concerning the L and SL components read, respectively (*cf.* Notation):

$$\dot{m}P_0(d_i)\Delta d + \frac{R_{i+1,L}W_{i+1,L}}{\Delta d} + \sum_{j=i+1}^{n} k_{a,L}U\frac{W_{j,L}}{d_j}P_{a,L}(d_i)\Delta d = \frac{R_{i,L}W_{i,L}}{\Delta d} + e_{i,L} + a_{i,L} + b_{i,L} + kC_{SO_2}W_{i,L} \quad (1)$$

$$\frac{kC_{SO_2}W_{i,L}}{MW_L}[(1-X_{S,i})MW_L + X_{S,i}MW_{SL}] + \frac{R_{i+1,SL}W_{i+1,SL}}{\Delta d} + \sum_{j=i+1}^{n} k_{a,SL}U\frac{W_{j,SL}}{d_j}P_{a,SL}(d_i)\Delta d = \quad (2)$$

$$= \frac{R_{i,SL}W_{i,SL}}{\Delta d} + e_{i,SL} + a_{i,SL} + b_{i,SL}$$

In Eq. (1), at LHS three inlet terms can be found, namely *i)* a term related to the feeding; *ii)* a term related to continuous particle shrinkage, where:

$$R = k_a U/3 \quad (3)$$

and *iii)* a term under summation, which takes into account particles formerly belonging to coarser particle size bins that fall into the i-th size bin due to attrition/fragmentation. At RHS, five outlet terms can be found, namely:

i) a term related to continuous particle shrinkage;

ii) a term related to sorbent loss by elutriation at the cyclone:

$$e_{i,L} = [1-\eta(d_i)]g_{i,L} \quad (4)$$

where $g_{i,L}$ is computed as a function of $W_{i,L}$ according to (14) and the cyclone collection efficiency is expressed as (*cf.* (15)):

$$\eta(d_i) = 1/[1+(d_{cut}/d_i)^c] \text{ for } d_i<120\ \mu m, \text{ otherwise } \eta=1 \quad (5)$$

iii) a term related to attrition/fragmentation, where:

$$a_{i,L} = k_{a,L}UW_{i,L}/d_i \quad (6)$$

iv) a term related to the bed drain where, according to the hypothesis of perfect mixing of bed material in the bottom bed, it is:

$$b_{i,L}/b = W_{i,L}/W \quad (7)$$

v) a term related to the transfer from the L to the SL phase, driven by the sulphation kinetics.

Equation (2) can be written taking into account that, for particles sulphated according to a core-shell pattern, it is:

$$X_{S,i} = X_S^{shell}[d_i^3 - (d_i - 2\delta)^3]/d_i^3 \quad (8)$$

for $d_i>2\delta$, otherwise $X_{S,i} = X_S^{shell}$. In particular, it has been discussed (16,17) that sorbent sulphation in FBC takes place in two subsequent stages: *stage I*, associated with the initial build-up of a sulphate-rich particle shell, and *stage II*, associated with

attrition-enhanced sulphation promoted by continuous attrition of sulphated material. Accordingly, the SO_2 capture efficiency can be calculated as:

$$\eta_{des} = F_{SO_2}^{cap} / F_{SO_2}^{inlet} = [kC_{SO_2} \sum_{i=1}^{n} (W_{i,L} X_{S,i}) / MW_L] / [\dot{m} / (MW_L r_{Ca/S})] \quad (9)$$

where the contribution to SO_2 capture given by stage II is assumed negligible, based on preliminary model computations. Finally, the SO_2 concentration is calculated as:

$$C_{SO_2} = C_{SO_2}^{inlet} (1 - \eta_{des}) \quad (10)$$

RESULTS AND DISCUSSION

Evaluation of Model Parameters

The model was solved in MATLAB™ environment, assuming typical values for the input parameters as reported in *Table 2*. In particular, the total bed inventory in the riser per unit cross-sectional area has been set at 800 kg m^{-2}, a typical figure based on admissible pressure drops across the riser in practical operation of CFBC. Based on realistic sorbent feeding rates and fuel ash content, it is further assumed that the total bed inventory consists of W=250 kg m^{-2} of sorbent (either L or SL) and 550 kg m^{-2} of fuel ash. Furthermore, P_0 was expressed as a log-normal distribution extending to the particle size range 5-2000 μm, with a mean particle size of 110 μm, about 28% of particles finer than 100 μm and about 4% of particles coarser than 1000 μm. The size distribution of attrited fines P_a was expressed as an exponential function for both L and SL:

$$P_{a,L}(d_i) = P_{a,SL}(d_i) = (1/\bar{d}) \exp(-d_i / \bar{d}) \quad (11)$$

with $\bar{d}$=35 μm. Attrition/fragmentation was considered to be active for particles coarser than 50 μm, while for finer particles its contribution was supposed to be negligible ($k_{a,L}$=$k_{a,SL}$=0). Moreover, the values of $k_{a,L}$ and $k_{a,SL}$ take into account both attrition by surface wear (3) and impact fragmentation (10). This latter contribution was calculated by estimating the fractional mass of fragments formed upon multiple particle impacts in the jetting region of a typical full-scale CFBC. The entrainment rate of sorbent particles into the jets, required to calculate the frequency and kinetic energy of impacts, has been estimated according to Massimilla (18). Finally, attrition in the cyclone has been neglected.

***Table 2*. Main input parameters of the model.**

$\dot{m}$	0.013 kg m^{-2} s^{-1}	c	4
$k_{a,L}$	5×10^{-9}	k	10^{-6} ppm^{-1} s^{-1}
$k_{a,SL}$	10^{-9}	X_S^{shell}	0.55
U	2.5 m s^{-1}	δ	50 μm
W	250 kg m^{-2}	$r_{Ca/S}$	2.5
d_{cut}	10 μm	$C_{SO_2}^{inlet}$	2000 ppm

Model Results

The influence of attrition on the combustor's performance has been assessed by comparing results obtained from computations performed neglecting attrition (*i.e.*, k_a=0 for both L and SL) with those in which attrition was considered. Results of computations for the no-attrition case are reported in *Figure 2* and *Table 3*. *Figure 2a* shows the probability density functions (PDF) of particle sizes, whereas the distribution is reported as cumulative undersize in *Figure 2b*. A noticeable shift toward coarser particles can be observed for material reporting to bottom ashes as compared with the lime feeding. The PDF peak is located at 120 μm, particles finer than 50 μm are hardly found and only 7% of particles mass is finer than 100 μm. On the other hand, the PDF peak is located at 65 μm in the population reporting to the fly ash: particles coarser than 120 μm are not present, 95% of particles mass is finer than 100 μm and the mean Sauter diameter is 48 μm. These values are critically dependent on cyclone efficiency characteristics. Values reported in *Table 3* show that sorbent reporting to fly ashes accounts for 21% of the total sorbent ashes even without attrition, due to the presence of elutriable fines in the sorbent feeding. The inventory of lime (W_L) is 22 kg m^{-2}, corresponding to 8.8% of the total sorbent inventory. Sulphur capture corresponds to η_{des}=0.78 when attrition is neglected.

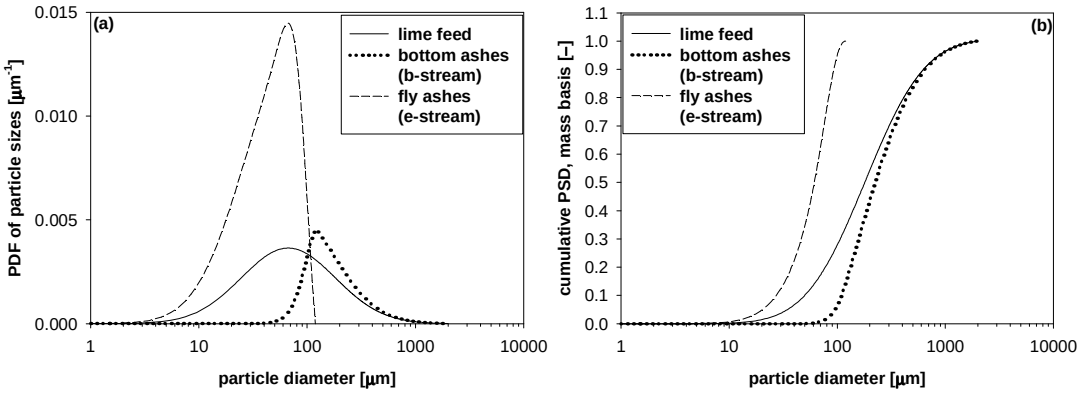

Figure 2. **Model results without attrition: (a) Probability density functions (PDF) of particle sizes for lime feed, bottom and fly ashes; (b) Cumulative particle size distributions (PSD) for lime feed, bottom and fly ashes.**

Table 3**. Selected output parameters of the model.**

	f [-]	W_L [kg m^{-2}]	W_{SL} [kg m^{-2}]	d_S for fly ashes [μm]	η_{des} [-]
Without attrition	0.21	22	228	48	0.78
With attrition	0.38	18	232	34	0.74
With attrition ($k_{a,L}$*3)	0.43	13	237	31	0.68
With attrition ($k_{a,L}$*10)	0.53	8	242	28	0.54

Model results considering the effect of attrition are reported in *Figure 3* and *Table 3*. Plots in *Figure 3* display the same general features of those corresponding to the no-attrition case. However it can be recognized that attrition/fragmentation induce a pronounced shift of the curves toward finer particle sizes. The PDF peaks are located at 115 μm and 55 μm for bottom and fly ashes, respectively. The fractional

mass of sorbent finer than 100 μm is 8% and 97% for bottom and fly ashes, respectively. The mean Sauter diameter of sorbent reporting to fly ashes is d_S=34 μm. As expected, consideration of attrition brings about an increase of the fractional mass of sorbent reporting to the fly ash (f raises to 0.38) and a decrease of W_L (18 kg m^{-2}, that is 7.2% of the total sorbent inventory). Correspondingly, W_{SL} increases due to the fact that attrition of L particles determines finer L-particle sizes and, in turn, a better Ca exploitation for SO_2 capture (*cf.* Eq. (8)). It is noteworthy that this feature does not imply an improvement in η_{des}, which decreases from 78% to 74%. This finding should be related to the competing effects of the better Ca exploitation in fine particles, on the one hand, and of the larger amount of material which is lost at the cyclone, on the other, when attrition/fragmentation are at work. Under the operating conditions selected in this work, the negative effect associated with fine sorbent loss at the cyclone overweighs the positive effect of a more extensive degree of calcium exploitation, resulting into a worse SO_2 abatement efficiency.

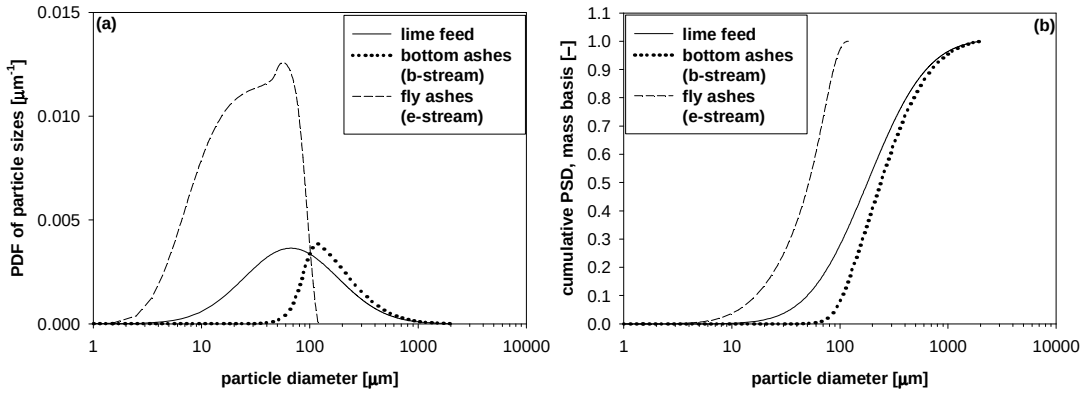

Figure 3. **Model results with attrition: (a) Probability density functions (PDF) of particle sizes for lime feed, bottom and fly ashes; (b) Cumulative particle size distributions (PSD) for lime feed, bottom and fly ashes.**

A sensitivity analysis has been carried out with reference to the attrition/fragmentation constant for L particles ($k_{a,L}$). In fact, while the value assumed for $k_{a,SL}$ (*cf. Table 2*) is to be considered as an upper limit for typical sorbents and operating conditions, the higher comminution susceptibility of L particles makes it possible to consider $k_{a,L}$-values also greater than the one reported in *Table 2*. Thus, *Table 3* lists the main results obtained when, holding all the other operating conditions/parameters, $k_{a,L}$ was increased by a factor of either 3 or 10. The model sensitivity was appreciable: as expected, enhanced attrition gives rise to increased f-values (up to 53%), decreased W_L-values (down to 8 kg m^{-2}) and decreased d_S-values for fly ashes (down to 28 μm). The overall detrimental influence that attrition/fragmentation do have on η_{des} is again highlighted: η_{des} is as low as 54% when $k_{a,L}$ was 10-times increased.

CONCLUSIVE REMARKS

The influence of particle attrition/fragmentation on sorbent inventory and particle size distribution in air-blown circulating fluidized bed combustors was carefully investigated by solving a population balance model able to take into account attrition and fragmentation phenomena, generation of fly and bottom ashes, kinetic aspects related to the SO_2 capture by lime-based sorbent particles. With reference to a base-case in which attrition was deliberately neglected, it was clearly shown that the presence of attrition ends up into increased fly ash amounts having finer mean particle sizes and decreased lime inventories in the bottom bed. Interestingly, the desulphurization ability of the system decreased since the effect related to the greater amount of material lost at the cyclone seemed to overweigh the effect related to a better calcium exploitation for SO_2 capture when finer particles are considered. The sensitivity of the model with reference to attrition/fragmentation constants appeared to be noticeable. Altogether, model computations confirmed the relevance of attrition and fragmentation to the performance of circulating fluidized bed combustors.

NOTATION

a	attrition rate [kg m^{-2} s^{-1}]
b	overall mass rate of sorbent bed drain [kg m^{-2} s^{-1}]
c	exponent appearing in Eq. (5) [-]
C_{SO_2}	SO_2 concentration [ppm]
$C_{SO_2}^{inlet}$	SO_2 inlet concentration [ppm]
Δd	particle diameter interval [m]
δ	thickness of the sulphated shell [m]
d	particle diameter [m]
$\bar{d}$	mean diameter of attrited fragments [m]
d_{cut}	cyclone cut diameter [m]
d_S	mean Sauter diameter [m]
η	cyclone collection efficiency [-]
η_{des}	SO_2 abatement efficiency [-]
e	overall mass rate of sorbent lost by elutriation [kg m^{-2} s^{-1}]
f	ratio e/(e+b) [-]
$F_{SO_2}^{cap}$	molar rate of SO_2 captured by the sorbent [kgmol m^{-2} s^{-1}]
$F_{SO_2}^{inlet}$	molar rate of SO_2 at the inlet [kgmol m^{-2} s^{-1}]
g	overall net mass rate along the riser of sorbent material [kg m^{-2} s^{-1}]
k	sulphation kinetic constant [ppm^{-1} s^{-1}]
k_a	attrition/fragmentation constant [-]
$\dot{m}$	overall mass feed rate of lime particles [kg m^{-2} s^{-1}]
MW	molecular weight [kg $kgmol^{-1}$]
P_0	particle size distribution of lime after primary fragmentation [m^{-1}]
P_a	particle size distribution of attrited fragments [m^{-1}]
R	rate of particle shrinkage due to attrition/fragmentation [m s^{-1}]
$r_{Ca/S}$	calcium to sulphur inlet molar ratio [-]
U	gas superficial velocity in the primary region of the riser [m s^{-1}]

W overall mass of sorbent in the bottom bed [kg m^{-2}]
X_S sulphation degree [-]
X_S^{shell} sulphation degree in the sulphated shell [-]

Subscripts

i, j, n referred to particles in the i-th, j-th, last (coarsest) size bin
L referred to lime particles
SL referred to sulphated limestone particles

REFERENCES

[1]. Chandran, R.R., Duqum, J.N.: Fluidization VI (Grace, J.R., Shemilt, L.W., Bergougnou, M.A., eds), Engineering Foundation New York (1989), pp. 571-580.
[2]. Couturier, M.F., Karidio, I., Steward, F.R.: Circulating Fluidized Bed Technology IV (Avidan, A.A., ed), American Institution of Chemical Engineers New York (1993), pp. 672-678.
[3]. Scala, F., Cammarota, A., Chirone, R., Salatino, P.: AIChE J. 43 (1997), pp. 363-373.
[4]. Di Benedetto, A., Salatino, P.: Powder Technol. 95 (1998), pp. 119-128.
[5]. Scala, F., Salatino, P., Boerefijn, R., Ghadiri, M.: Powder Technol. 107 (2000), pp. 153-167.
[6]. Montagnaro, F., Salatino, P., Scala, F.: Combust. Sci. and Tech. 174 (2002), pp. 151-169.
[7]. Werther, J., Reppenhagen, J.: Handbook of Fluidization and Fluid-Particle Systems (Yang, W.C., ed), Dekker New York (2003), pp. 201-237.
[8]. Chen, Z., Lim, J., Grace, J.R.: Chem. Eng. Sci. 62 (2007), pp. 867-877.
[9]. Saastamoinen, J.J., Shimizu, T.: Ind. Eng. Chem. Res. 46 (2007), pp. 1079-1090.
[10]. Scala, F., Montagnaro, F., Salatino, P.: Energy Fuels 21 (2007), pp. 2566-2572.
[11]. Montagnaro, F., Salatino, P., Scala, F., Chirone, R.: Powder Technol. 180 (2008), pp. 129-134.
[12]. Scala, F., Montagnaro, F., Salatino, P.: Can. J. Chem. Eng. 86 (2008), pp. 347-355.
[13]. Shimizu, T., Saastamoinen, J.: 20th Int. Conf. FBC (Yue, G., Zhang, H., Zhao, C., Luo, Z., eds), Xi'an (2009), pp. 1028-1034.
[14]. Wirth, K.E.: Chem. Eng. Technol. 14 (1991), pp. 29-38.
[15]. Redemann, K., Hartge, E.-U., Werther, J.: Powder Technol. 191 (2009), pp. 78-90.
[16]. Shimizu, T., Peglow, M., Sakuno, S., Misawa, N., Suzuki, N., Ueda, H., Sasatsu, H., Gotou, H.: Chem. Eng. Sci. 56 (2001), pp. 6719-6728.
[17]. Scala, F., Salatino, P.: Chem. Eng. Technol. 32 (2009), pp. 380-385.
[18]. Massimilla, L.: Fluidization II (Davidson, J.F., Clift, R., Harrison, D., eds), Academic Press London (1985), pp. 133-172.